International Journal of GEOMATE, Oct., 2020, Vol.19, Issue 74, pp.176–184
ISSN: 2186-2982 (P), 2186-2990 (O), Japan, DOI: https://doi.org/10.21660/2020.74.72565
Geotechnique, Construction Materials and Environment

A NEURAL NETWORK APPROACH FOR PREDICTING HARDENED PROPERTY OF GEOPOLYMER CONCRETE

Tung Thanh Pham[1], *Tu Trung Nguyen[2], Linh Ngoc Nguyen[3], and Phuong Viet Nguyen[4]

[1,3] Faculty of Building and Industrial Construction, National University of Civil Engineering, Vietnam.
[2] Facuty of Civil Engineering Department, Hanoi Architectural University, Vietnam.
[4]Faculty of Bridge and Roads, National University of Civil Engineering, Vietnam

*Corresponding Author, Received: 30 May 2020, Revised: 10 June 2020, Accepted: 24 June 2020

ABSTRACT: This paper presents the application of an Artificial Neural Network (ANN) approach to predict the 28-day compression strength of Geopolymer concrete (GPC) from the input ingredients. A total of 190 test samples collected from previously published were employed for training and validating the ANN model. Additionally, a test project was also implemented to collect the experimental data for verifying the prediction ability of the ANN model. Different learning algorithms were investigated to obtain the optimal algorithm for the GPC data. Results from the study revealed that the ANN model using the "trainlm" learning algorithm provided the best prediction results. The average prediction error about 8 MPa was found for the unseen data set. Besides, the effects of changing input variables to the output of the model were also explored by conducting the sensitivity analysis. It was shown that the 28-day GPC compression strength was more sensitive to the change of coarse aggregate (CoAg) and sodium silicate (Na_2SiO_3) variables.

Keywords: Geopolymer Concrete (GPC); Compression Strength; Artificial Neural Networks (ANN); Sensitivity Analysis.

1. INTRODUCTION

Conventional concrete using Ordinary Portland cement (OPC) as the primary binder is one of the widely employed materials all over the world. However, the production of OPC consumes a substantial amount of natural resources. It emits a significant volume of carbon dioxide to the air, leading to a severe impact on the global environment. According to a study of Malhotra [1], the entire cement industry annually releases about 7% of the total human-made (around 2.8 billion tons) of the greenhouse gas to the atmosphere. A feasible solution to reduce the adverse effects for the environment in the production of the conventional concrete is to replace OPC with by-product or geological origin materials. This leads to the development of a new type of concrete called Geopolymer concrete.

Geopolymer concrete (GPC) is an environmentally friendly material that uses fly ash to replace cement as the primary binder. Fly ash is a by-product material from power plants containing aluminous and siliceous ingredients. Geopolymer concrete is a promising alternative candidate to replace OPC in providing sustainable material with excellent resistance for the chemical attack and fire performance [2,3]. According to Davidovits [4], geopolymer paste is formed by the chain and ring polymers with Si^{4+} and Al^{3+} in IV-fold coordination with oxygen (polysilanes). The empirical formula of polysilanes is presented as below

$$M_n\,(-(SiO_2)_z - AlO_2)_n \,.\, wH_2O \qquad (1)$$

where "z" is 1, 2, or 3 or higher up to 32; M is a monovalent cation such as potassium or sodium, and "n" is a degree of polycondensation [4].

Geopolymer production is required for rich alumino-silicate materials and alkaline solutions. The material with rich in silicon (Si) and aluminum (Al) content may come from natural sources such as kaolinite, clays, and micas or the by-product material, including fly ash, silica fume, slag. The alkaline liquids can be obtained from solvable alkali metals that such as Sodium or Potassium based. Intensive research has been conducted to explore the effects of ingredients on the GPC compressive strength. For example, Xu and Van Deventer [5] stated in their study that the GPC using potassium hydroxide as the alkaline liquids produced a better compressive strength than that of sodium hydroxide.

In another study, Palomo et al. [6] investigated various combinations of alkaline liquids. The conclusion from the study revealed that among different combinations, a mixture of sodium silicate and sodium hydroxide could result in the highest compressive strength of GPC. Related to the effects of calcium content in by-product materials to the compressive strength of GPC, Gourley [7] recommended in his study that the GPC using materials with low calcium (ASTM Class F) would provide a higher compression strength compared to that of the materials with high calcium (ASTM Class C).

Traditionally, the experimental method is often used to determine the compression strength and other properties of different materials [8-11]. This method provides the compression strength of concrete with a high level of accuracy. However, this technique is destructive and time-consuming. Recently, an alternative approach using Artificial Intelligence (AI) to predict the strength of materials has been broadly employed. This novel technique involves two steps. In the first step, the approach using the available experimental data to establish the relationship between the input variables and outputs. In the second step, the successfully established connections are then applied to predict the outputs of an unseen input dataset.

In a recent study, Dao et al. [12] used two AI-based approaches, namely Adaptive Neuro-Fuzzy Inference (ANFIS) and Artificial Neural Network (ANN) to predict the compression strength of GPC. Four parameters, namely Fly Ash, Na_2SiO_3, NaOH, and H_2O, were utilized as the inputs of the model, and the 28-day compression strength of GPC was used as the output. A total of 210 data samples were employed for training, validation, and testing the proposed models. The results from the study revealed that the models showed strong potential for the prediction of the GPC compression strength.

Besides the applications for estimating the compression strength of GPC, the AI-based approaches were also used to tackle various engineering topics. For instance, in the study of Nguyen and Dinh [13], and Nguyen et al. [14], the AI-based methods were applied to predict the compression strength of conventional and high-performance concrete. Other researchers applied AI-based technique to identify structural damage [15], to estimate fire resistance ratings for wood structures [16], to predict the ultimate shear strength of steel fiber reinforced concrete [17], to predict the bridge desk rating [18], to predict the compression strength of the different types of concrete [19,20], or to optimize the performance in the wastewater treatment plant [21].

AI-based methods were also popular among researchers recently. As an example, Truong et al. [22] employed different AI-based approaches to evaluate the safety of steel trusses. The finding of the study revealed that the Gradient Tree Boosting algorithm provided the best performance. Elevado et al. [23] applied k-nearest neighbor model to predict the compression strength of the concrete made of fly ash and waste ceramics. Results from the study showed an acceptable prediction capacity of the model.

In this study, a supervised learning model using the ANN technique was developed to predict the compression strength of GPC concrete at 28 days old. The structure of the ANN model was built in MATLAB R2020a Runtime Environment with six input variables and one output. Two steps involving different datasets were performed to create the ANN model. In the first step, the ANN model was trained and validated using available data collected from the previous publications. In the second step, experimental work was implemented in the lab to collect the experimental dataset for verifying the prediction capacity of the proposed ANN model. The 28-day GPC compression strength collected from the destructive tests of specimens were compared to the non-destructive compression strength data generated from the proposed ANN model.

2. DATA PREPARATION

2.1 Experimental Data

A series of nine GPC specimens were fabricated and tested in the lab at the National of Civil Engineering University to collect the GPC 28-day compression strength. Three GPC mixtures with the ratio of alkaline activator over the paste varied from six to ten were used to cast specimens. All specimens were cured in the water in 28 days before conducting the compression tests. Details of material components, mixtures, specimen preparation, and data collection are presented in the subsequent sections.

2.1.1 Materials

Fly Ash (FA) was collected from the Pha Lai coal-fired power station in the Northern part of Vietnam was used in this study. The average particle diameter of FA is 15.5μm. Another by-product material, Blast Furnace Slag (BFS), gathering from the Thai Nguyen Steel factory, was also utilized along with FA as the cement replacement material. The specific surface area by Blaine of BSF is 4520 cm^2/g, with an average diameter of 7.63μm. The chemical composition of FA and BSF in terms of percentage by mass is listed in Table 1

Table 1 Chemical composition of FA and BFS

Oxides	SiO_2	Al_2O_3	Fe_2O_3	CaO	MgO	K_2O	Na_2O	SO_3	TiO_2
FA (%)	57.3	25.2	6.06	1.09	1.68	5.29	0.16	0.09	0.83
BFS (%)	43.7	12.9	1.47	28.7	6.29	1.22	0	1.35	0.84

The sodium silicate (Na_2SiO_3) was used as the alkaline activator for producing GPC in this study. The amount of alkaline activator was calculated to ensure the ratio of SiO_2/Al_2O_3 in the input ingredients maintains between two to three. Natural crushed rock with a maximum size of 10 mm was selected for coarse aggregate. The natural sand with a particle size less than 5 mm was chosen for fine aggregate. Details of sieve analysis followed by TCVN 7572-2 [24] are presented in Table 2.

Table 2 Sieve analysis results

Type of agg.	Sieve size (mm)	Cumulative retained (%)	Standards
Coarse	40	0	TCVN 7572-2
	20	8.2	
	10	50.3	
	5	95.5	
	< 5	100	
Fine	5	0	
	2.5	8	
	1.25	27.6	
	0.63	52.3	
	0.315	78.4	

2.1.2 Mixture proportions and specimen preparation

Table 3 presents the composition of three GPC mixtures. The ratio of alkaline activator over the paste (FA and BSF) in the mixture of MIX1, MIX2, and MIX3 was six, eight, and ten percent, respectively. For each mixture, a set of three specimens using a standard cube with the dimensions of 150×150×150 mm was cast. These specimens were then cured in water for 28 days until the compression tests were implemented.

2.1.3 Experimental data collection

The compression tests conformed to the requirements of TCVN 3118 [25] were conducted at LAS XD125 – National of Civil Engineering University using the AD200/EL Unit test machine. The maximum compression capacity of the testing equipment is 2000 kN. The compression tests were implemented with the constant loading speed of 70kN/10s until the test specimen was failed. The maximum force for each specimen was documented. Table 3 shows the compression strength of the GPC specimens.

2.2 Data from Previous Study

Information of seven GPC properties, namely Furnace ash (FAsh), Coarse aggregate (CoAg), Fine aggregate (FiAg), Sodium hydroxide solution (NaOH), Sodium silicate (Na_2SiO_3), Water (H_2O), and GPC 28-day compression strength (fc'_{28}) was collected from the previously published research [26, 27]. Data of the 190 test samples were then employed to train and validate the proposed ANN model. The characteristics of the data are presented in Table 4. Detailed information is presented in Appendix A. Note that the difference in the range of the input data was found not quite large, Thus, the normalization step was not performed for the input.

Table 3 Mix proportions and compression strength of test samples

No.	Mixture	Test Sample	FAsh (kg)	CoAg (kg)	FiAg (kg)	NaOH (kg)	Na_2SiO_3 (kg)	H_2O (kg)	fc'_{28} (MPa)
1	MIX1	1	520	1050	760	25	31.2	240	38
2		2	520	1050	760	25	31.2	240	41
3		3	520	1050	760	25	31.2	240	38
4	MIX2	1	520	1050	760	30	41.6	240	43
5		2	520	1050	760	30	41.6	240	46
6		3	520	1050	760	30	41.6	240	45
7	MIX3	1	520	1050	760	45	52	240	54.2
8		2	520	1050	760	45	52	240	56
9		3	520	1050	760	45	52	240	52.1

Table 4 Characteristics of data from previously published

No.	FAsh (kg)	CoAg (kg)	FiAg (kg)	NaOH (kg)	Na_2SiO_3 (kg)	H_2O (kg)	fc'_{28} (MPa)
1	350	1200	645	41	103	35	20
2	428	1170	630	57	114	86	20
3	400	950	850	57	143	80	22.6

-	-	-	-	-	-	-	-
-	-	-	-	-	-	-	-
188	408	1294	554	41	103	22.5	45
189	408	1294	554	41	103	0	58
190	408	1201	647	62	93	4	32
Min.	254.5	723	535	22.77	48	0	20
Max.	498.5	1772	850	120	144	113.6	89

3. ARTIFICIAL NEURAL NETWORK APPROACH

3.1 ANN Structures

An ANN structure is a supervised learning system that mimics the operation of the human brain. The typical shallow ANN system often consists of an input layer, a hidden layer, and an output layer. Each layer includes one or several inter-layers connected processing units, also known as a neuron. Fig.1 depicts the structure of a typical ANN system. The neurons in the hidden layer are linked to the neurons of adjacent layers (input and output layer) through the adjustable weighting factor (w_{ij}). The value of the factor would be adjusted during the network training process to obtain the best relationship between input and output variables.

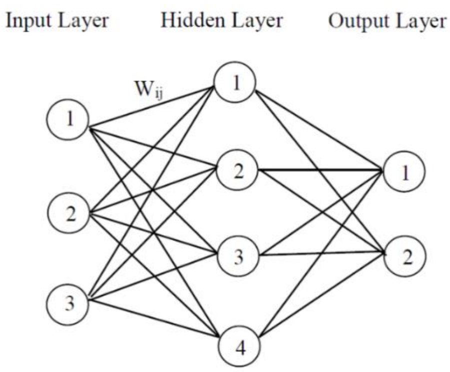

Fig.1 Structure of a typical ANN system

Of all the popular training algorithm, the backward propagation of errors, or backpropagation, is the most widely used for the supervised learning ANN system. This algorithm consists of two reverse stages, called forward and backward stage. In the first stage, an arbitrary weight value is assigned for each connection in the entire network to establish the initial connection between input and output. In the second phase or backward phase, the difference (error) between the actual and the desired output is calculated and propagated back into the network. The connection weight is adjusted during these iterative processes to minimize the input and output error.

3.2 Model Assessment

Performances of the ANN model was assessed based on three factors: coefficient of determination (R^2), Mean Squared Error (*MSE*), and Root Mean Squared Error (*RMSE*). The coefficient of determination measures the correlation between input and output parameters using eq. (2)

$$R^2 = 1 - \frac{\sum_{i=1}^{n}(y_i-\hat{y}_i)^2}{\sum_{i=1}^{n}(y_i-\bar{y})^2} \quad (2)$$

where y_i is the i^{th} actual output, $\bar{y}$ is the mean of the actual outputs, $\hat{y}_i$ is the i^{th} predicted outputs, and n is the total number of data samples. *MSE* is the average squared difference between predicted outputs and actual outputs. *MSE* can be computed using eq. (3)

$$MSE = \frac{1}{n}\sum_{i=1}^{n}(y_i - \hat{y}_i)^2 \quad (3)$$

Root Mean Squared Error is the square root of Mean Squared Error and can be calculated by eq. (4)

$$RMSE = \sqrt{\frac{1}{n}\sum_{i=1}^{n}(y_i - \hat{y}_i)^2} \quad (4)$$

3.3 Model Development

Six parameters, including FAsh, CoAg, FiAg, NaOH, Na_2SiO_3, and H_2O were selected as the input variables for the ANN model, and the GPC 28-day compression strength (fc'_{28}) was designated as the output. The dataset from the previous studies was randomly divided into two subsets in which 85% (i.e., 160 data points) of the entire dataset was employed for training model, 15% (i.e., 30 data points) for validation. The experimental dataset with 9 data samples was utilized for testing the prediction accuracy of the ANN model.

Multiple learning algorithms with variations of neuron numbers in the hidden layer were investigated in this study. The purpose of these tasks was to obtain the optimal ANN model for the GPC data. The performance of the ANN model was evaluated based on the *MSE* value. For each model configuration, the potential model was run for 10 trials to find the best performance result for both training and validation datasets. Figure 2a shows the performance of the ANN models with different learning algorithms. The performance of the ANN models with changing neuron numbers in the hidden layer from one to 20 is presented in Fig.2b.

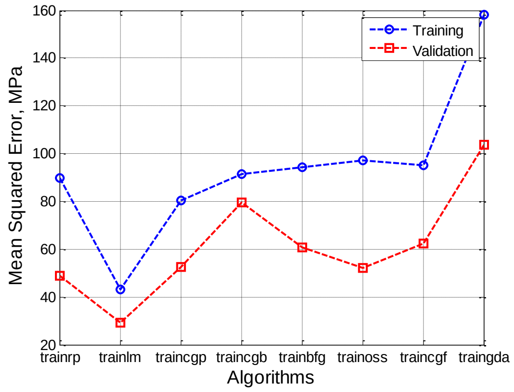

(a) Different learning algorithms

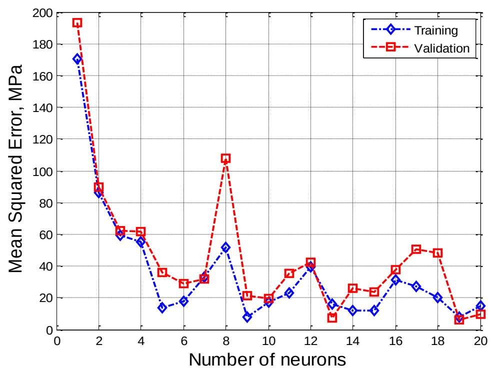

(b) Variation of neuron numbers

Fig 2 Performance of potential ANN models

As can be seen clearly in Fig.2a, the 'trainlm' (Levenberg-Marquardt) algorithm generated the best performance result for the proposed ANN model. The outcome was in line with the previous study [15]. Additionally, the ANN model with 19 neurons in the hidden layer was found to produce optimal performance results, as presented in Fig. 2b. Other information about the selected ANN model to employ in this study is listed in detail in Table 5.

Table 5 Details of the selected ANN model

Parameter	Information
# neurons in the input layer	6
# neurons in hidden layer	19
# neurons in the output layer	1
Training method	backpropagation
Learning algorithm	trainlm
Activation function	sigmoid

4. RESULTS AND DISCUSSIONS

4.1 Model Performance

As mentioned above, the proposed ANN model was trained and validated with the dataset collected from previously published research. Three indicators, namely, R^2, *MSE*, and *RMSE*, were employed to assess the performance of the ANN model. Table 6 lists the values of these indicators for the training dataset, validation dataset, and overall. As can be observed from the table, the ANN model performed well with a coefficient of determination was 0.7209 and 0.6192 for the training and validation dataset, respectively. It is worth noting that the larger value of R^2, the better the prediction capacity of the model.

Table 6 Performance results of ANN model

	Training	Validation	Overall
R^2	0.7209	0.6192	0.7047
MSE	81.71	73.93	80.56
RMSE	9.04	8.59	8.97
Samples	160	30	190

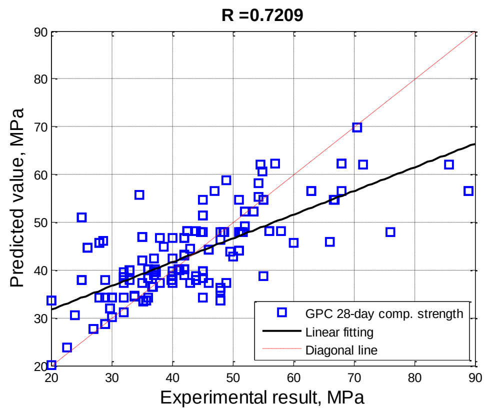

(a) Training

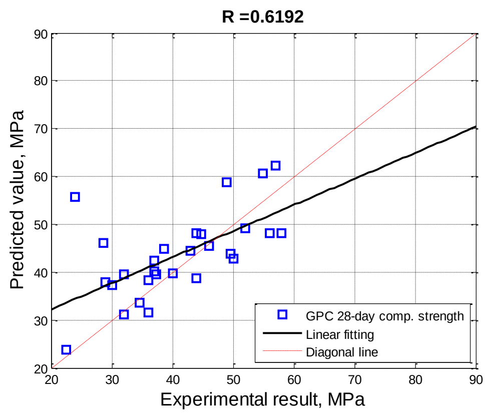

(b) Validation

Fig.3 Performance of selected ANN model

An alternative method to present the performance results of the ANN model is using regression plots. Fig.3 shows the performance results of the proposed ANN model for different datasets. In these figures, the horizontal axis represents the actual value, and the vertical axis represents the predicted values generated by the proposed ANN model. The samples located on the diagonal lines show an ideal prediction of the model.

4.2 Error Evaluation

The error histogram with 20 bins (columns) of the performance errors of the proposed ANN model is presented in Fig.4. The error was the difference between the predicted value produced by the ANN model and the actual value. In this figure, the vertical axis represents the number of samples from a dataset, while the horizontal axis presents the error corresponding to the bins. The zero-line is the zero error on the horizontal axis. As can be seen, most samples had errors between -7.56 MPa and 8.48 MPa. The negative errors indicated that the predicted value from the ANN model was smaller than the experimental one.

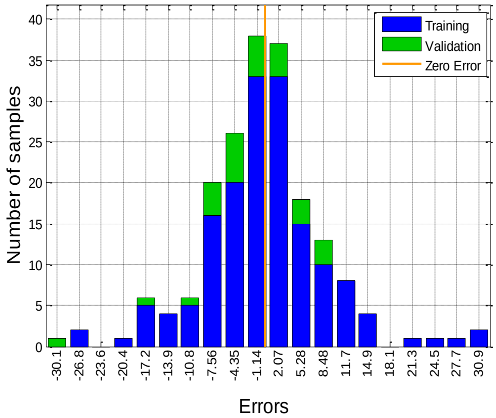

Fig.4 Error assessment for the selected ANN model

4.3 Application of Artificial Neural Network for Experimental Data

The successful ANN model was then employed to predict the compression strength of GPC. The input data for the model was the ingredients for mixtures, as presented in Table 3. The output of the model was the predicted GPC 28-day compressive strength. The compressive strength produced by the ANN model was then compared to the experimental compression strength obtained from the destructive tests. Table 7 presents the performance results of the model for the experimental data set.

As can be seen from Table 7, the ANN model performed reasonably well for the experimental dataset with an average error of about 8 MPa. It is worth pointing out that the experimental dataset was unseen for the proposed ANN model. The ANN model could predict the compressive strength of GPC in a wide range from 38 MPa to 56 MPa with an approximate error of 20 percent. That means the ANN model could generalize the nonlinear relationship between the inputs and output.

4.4 Sensitivity Analysis

The sensitivity analysis was conducted for each input variable by changing its value from low to high while keeping the value of others at the mid-value. To do that, the input data were divided into five groups including the Low (the smallest value of each input parameter), the Mid Low (a halfway from Low to Mid), the Mid (a halfway from Low to High), the Mid High (a halfway from Mid to High), and the High (the largest value of each input parameter), as listed detail in Table 8.

Table 7 Performance results for the proposed ANN model

No.	Experimental (MPa)	Predicted (MPa)	Error (MPa)	Error (%)
1	38.0	31.5	6.48	17.0
2	41.0	31.5	9.48	23.1
3	38.0	31.5	6.48	17.0
4	43.0	36.6	6.40	14.9
5	46.0	36.6	9.40	20.4
6	45.0	36.6	8.40	18.7
7	54.2	43.1	11.1	20.4
8	56.0	43.1	12.9	23.0
9	52.1	43.1	8.97	17.2

Table 8 Data for sensitivity analysis

	FAsh (kg)	CoAg (kg)	FiAg (kg)	NaOH (kg)	Na_2SiO_3 (kg)	H_2O (kg)
Low	254	723	535	22.8	48	0
Mid Low	315	985	614	47.1	72	28.4
Mid	376	1247	692	71.4	96	56.8
Mid High	437	1509	771	95.7	120	85.2
High	498	1772	850	120.0	144	114

Fig.5 presents the sensitivity analysis results of all input variables in the form of a parallel coordinate diagram. This graph has five vertical axes arranged from left to right along with the horizontal axis; each of the axes corresponds to a different level of the input parameters. The vertical axis represents the GPC 28-day compression strength. As can be observed clearly, the 28-day compression strength of GPC was responsive to the change of coarse aggregate and sodium silicate parameters.

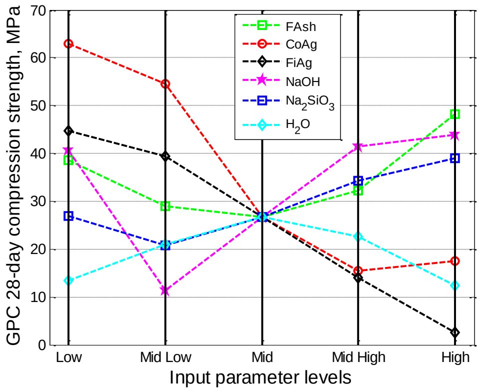

Fig.5 Sensitivity analysis result

4. CONCLUSIONS

The ANN technique was employed in this study to predict the compression strength of GPC at 28 days old. In the first stage, available data were utilized to develop the ANN model. In the second stage, experimental data was used to test the prediction capacity of the model. Performance results revealed that the ANN model could predict the wide range of output for the unseen experimental data with an error of around 20 percent. In addition, the “trainlm” learning algorithm was found to generate the best results for the proposed ANN model.

With respect to the sensitivity analysis, the outcomes indicated that the coarse aggregate (CoAg) and sodium silicate (Na_2SiO_3) were among the two input variables, which had a significant influence on the output parameter of the ANN model. Finally, it was concluded that the ANN model could be used as an alternative method to predict the compression strength of GPC with an acceptable level of accuracy.

5. ACKNOWLEDGMENT

This research is funded by the National University of Civil Engineering (NUCE), Hanoi, Vietnam under a grant number 29-2019/KHXD-TĐ. Any opinions, findings, and conclusions or recommendations expressed in this material are those of the authors and do not necessarily reflect the views of the NUCE.

6. REFERENCES

[1] Malhotra V.M., Introduction: Sustainable Development and Concrete Technology, ACI Concrete Journal, 2000, pp.1147-1165.
[2] Mehta A., and Siddique R., Sulfuric acid resistance of fly ash-based geopolymer concrete. Construction and Building Materials, 146, 2017, pp.136–143. https://doi.org/10.1016/j.conbuildmat.2017.04.077
[3] Kong D.L.Y., and Sanjayan J.G., Damage behavior of geopolymer composites exposed to elevated temperatures, Cement and Concrete Composites, Vol. 30, 2001, pp.986–991, https://doi.org/10.1016/j.cemconcomp.2008.08.001
[4] Davidovits J., Synthetic Mineral Polymer Compound of The Silicoaluminates Family and Preparation Process, United States Patent - 4,472,199, 1984, (pp.1-12). USA.
[5] Xu H., and Deventer J.S.J.V., The geopolymerisation of alumino-silicate minerals. International Journal of Mineral Processing, 59(3), 2000, pp.247-266.
[6] Palomo A., Grutzeck M.W., and BlancoM.T., Alkali-activated fly ashes A cement for the future. Cement and Concrete Research, 29(8), 1999, pp.1323-1329.
[7] Gourley J.T., Geopolymers; Opportunities for Environmentally Friendly Construction Materials. Paper presented at the Materials 2003 Conference: Adaptive Materials for a Modern Society, Sydney.2003.
[8] Nguyen T.T., Dao T.N., Aaleti S., Hossain K., and Fridley K.J., Numerical model for creep behavior of axially loaded CLT panels. *J. Struct. Eng.* 145:04018224. https://doi.org/10.1061/(ASCE)ST.1943-541X.0002219, 2019.
[9] Nguyen T.T., Phan Q.M., Pham T.T., Nguyen V.P., Experimental study on mechanical and hydraulic properties of porous Geopolymer concrete. International Journal of GEOMATE, Oct. 2020, Vol.19, Issue 74, pp.66–74. ISSN: 2186-2982 (P), 2186-2990 (O), Japan, DOI: https://doi.org/10.21660

/2020.74.41280
[10] Zatar, W., & Nguyen, T. T. (2020). Mixture Design Study of Fiber-Reinforced Self-Compacting Concrete for Prefabricated Street Light Post Structures. *Advances in Civil Engineering*, *2020*, 8852320. https://doi.org/10.1155/2020/8852320.
[11] Nguyen T.T., Modeling of CLT creep behavior and real-time hybrid simulation of a CLT-LiFS building (Doctoral dissertation, University of Alabama Libraries). 2017.
[12] Van Dao D., Ly H.B., Trinh S.H., Le T.T., and Pham B.T., Artificial intelligence approaches for prediction of compressive strength of geopolymer concrete. Materials, 12(6).
[13] Nguyen T.T., and Dinh K., An artificial intelligence approach for concrete hardened property estimation. Journal of Science and Technology in Civil Engineering (STCE) - NUCE, 14(2), 40-52. https://doi.org/10.31814/stce.nuce2020-14(2)-04, 2020.
[14] Nguyen T.T., Pham D. H., Pham T.T., and Vu H.H., Compressive strength evaluation of Fiber-Reinforced High Strength Self-Compacting Concrete with artificial intelligence. Manuscript submitted for publication, 2020
[15] Hung T.V., Viet V.Q., and Thuat D.V., A deep learning-based procedure for estimation of ultimate load carrying of steel trusses using advanced analysis. Journal of Science and Technology in Civil Engineering (STCE) - NUCE, 13(3), 113-123. https://doi.org/10.31814/stce.nuce2019-13(3)-11., 2019.
[16] Tung P.T., and Hung P.T., Predicting fire resistance ratings of timber structures using artificial neural networks. Journal of Science and Technology in Civil Engineering (STCE) - NUCE, 14(2), 28-39. https://doi.org/10.31814/stce.nuce2020-14(2)-03, 2020.
[17] Kanchan P., Amit K.G., Pramila G., Development of ANFIS models for air quality forecasting and input optimization for reducing the computational cost and time, Atmospheric Environment, Vol.128, ISSN 1352-2310, 2016.
[18] Nguyen T.T., and Dinh K., Prediction of bridge deck condition rating based on artificial neural networks. Journal of Science and Technology in Civil Engineering (STCE) - NUCE, 13(3), 15-25.https://doi.org/10.31814/stce.nuce2019-13(3)-02., 2019.
[19] Naderpour H., Rafiean A.H., and Fakharian P., Compressive strength prediction of environmentally friendly concrete using artificial neural networks. Journal of Building Engineering, 16(January), 213–219. https://doi.org/10.1016/j.jobe.2018.01.007, 2018.
[20] Ahmadi M., Naderpour H., and Kheyroddin A., ANN Model for Predicting the Compressive Strength of Circular Steel-Confined Concrete. International Journal of Civil Engineering, 15(2), 213–221. https://doi.org/10.1007/s40999-016-0096-0, 2017.
[21] Eugene H., Anteneh M.Y., Tushar K.S., Ha Ming A., and Ahmet K., ANFIS based Modelling of dewatering performance and polymer dose optimization in a wastewater treatment plant, Journal of Environmental Chemical Engineering, Vol.6, Issue 2, 2018.
[22] Truong V.H., Vu Q.V., Thai H.T., and Ha M.H., A robust method for safety evaluation of steel trusses using Gradient Tree Boosting algorithm. Advances in Engineering Software, 147, 102825. https://doi.org /10.1016/j.advengsoft.2020.102825, 2020.
[23] Elevado K.J.T., Galupino J.G., and Gallardo R.S., Compressive strength optimization of concrete mixed with waste ceramics and fly ash. International Journal of GEOMATE, 16(53), 135–140,2019.
[24] TCVN 7572-2 (2006), Aggregates for concrete and mortar – Test methods - Part 2: Determination of particle size distribution
[25] TCVN 3118, Heavyweight concrete - Method for determination of compressive strength, 1993.
[26] Hassan A., Arif M., and Shariq M., Use of geopolymer concrete for a cleaner and sustainable environment – A review of mechanical properties and microstructure. Journal of Cleaner Production, 223, 704–728, 2019.
[27] Wilson A., Establishing a Mix Design Procedure for Geopolymer Concrete. (Thesis, University of Southern Queensland), Australia,2015.

Appendix A Experimental data from the previous study

No.	FAsh (kg)	CoAg (kg)	FiAg (kg)	NaOH (kg)	Na_2SiO_3 (kg)	H_2O (kg)	fc'$_{28}$ (MPa)
1	350	1200	645	41	103	35	20
2	428	1170	630	57	114	86	20
3	400	950	850	57	143	80	22.5
4	380	1050	800	40	110	0	24
5	428	1170	630	57	114	64	24
6	400	1222	658	40	100	0	25
7	408	1243	554	41	103	20	25
8	400	1209	651	45.7	114.3	0	26
9	400	1222	658	56	84	0	27
10	408	1232	616	48	103	0	28
11	428	1170	630	49	122	43	28
12	428	1177	623	68.5	102.8	28.5	28.6
13	408	1246	554	41	103	20	29
14	408	1080	554	41	103	20	29
15	428	1170	630	49	122	43	29
16	394	1201	647	52.5	105.1	21.4	29.7
17	428	1170	630	49	122	43	30
18	444	1170	630	44	111	43	30
19	428	1170	630	49	122	43	30
20	428	1170	630	57	114	43	30
21	408	1294	554	41	103	21.3	32
22	408	1232	616	41	103	21.3	32
23	408	1201	647	62	93	4	32
24	428	1170	630	49	122	43	32
25	428	1170	630	49	122	43	32
26	428	1170	630	57	114	43	32
27	408	1243	554	41	103	20	33
28	408	1232	616	55.4	103	0	33
29	420.5	1032	555.7	37.6	80.1	113	33.7
30	378	1294	554	50	124	0	34.5
31	378	1772	554	50	124	0	34.6
32	408	1294	554	41	103	10.7	35
33	408	1232	616	41	103	10.6	35
34	428	1170	630	57	114	43	35
35	365.1	1118	602	34.3	73.0	103	35.2
36	408.8	1177	623	57.2	85.8	24.4	35.7
37	408	1294	554	51.5	103	16.5	36
38	408	1294	554	41	103	22.5	36
39	408	1201	647	62	93	0	36
40	428	1170	630	49	122	43	36
41	408	1294	554	41	103	22.5	36
42	254.5	1290	694.6	22.7	48.5	68.7	36.7
43	408	1201	647	41	103	20.7	37
44	406	1194	643	41	102	26.8	37
45	404	1190	640	41	102	25.5	37
46	480	1153	599	56	112	23.7	37.1
47	400	950	850	57	143	60	37.3
48	408	1201	647	41	103	14.3	38
49	428	1170	630	57	114	43	38

Continues to next page

Appendix A continues

50	444.4	1177	623	44.4	111.1	18.6	38.7
51	498.4	1153	599	59.8	89.7	26.5	39.9
52	408	1201	647	41	103	14.3	40
53	408	1201	647	41	103	20.7	40
54	408	1201	647	41	103	26.5	40
55	408	1294	554	41	103	16.5	40
56	428	1170	630	57	114	43	40
57	408	1294	554	51.5	103	16.5	41
58	408	1294	554	51.5	103	16.5	41
59	408	1232	616	55.4	103	0	41.2
60	408	1294	554	51.5	103	16.5	42
61	408	1201	647	41	103	14.4	42
62	309.8	1204	648.3	27.7	59.1	83.6	42
63	408	1202	647	41	103	26	42
64	461.5	1177	623	46.2	92.3	18.6	42.5
65	408	1201	647	41	103	17.6	43
66	428	1170	630	57	114	43	43
67	408	1294	554	41	103	0	44
68	408	1201	647	55.4	103	0	44
69	400	1265	540	42.3	105.7	24.3	44
70	400	950	850	57	143	48	44.8
71	408	1201	647	41	103	7.5	45
72	408	1232	616	41	103	20.7	45
73	408	1232	616	41	103	0	45
74	408	1294	554	41	103	22.5	45
75	428	1170	630	49	122	43	45
76	408	1294	554	41	103	22.5	45
77	400	950	850	57	143	48	45.0
78	405	1235	545	52.9	132.4	28	46
79	404	1190	640	41	102	17	46
80	428	1170	630	57	114	43	46
81	428	1170	630	57	114	43	46
82	408	1201	647	41	103	0	47
83	400	950	850	57	143	48	47.9
84	476	1294	554	120	48	0	48
85	408	1232	616	41	103	26.5	48
86	350	1200	645	41	103	35	48
87	408	1201	647	68	103	0	48
88	400	950	850	57	144	48	48.5
89	400	950	850	57	143	48	48.5
90	380	1233	540	56.5	141.3	14.6	49
91	428	1170	630	57	114	43	49
92	462.8	1153	599	52.9	132.2	21.2	49.6
93	404	1195	640	41	102	20	50
94	408	1232	616	41	103	14.4	51
95	408	1232	616	41	103	0	51
96	400	950	850	57	143	48	51.0
97	400	950	850	57	143	48	51.4
98	400	950	850	57	143	48	51.6
99	408	1232	616	41	103	7.5	52
100	400	1356	535	51.5	128.6	12.7	52
101	400	950	850	57	143	40	53.4
102	408	1201	647	63	138	0	54.2
103	408	723	647	63	138	0	54.2
104	368	1294	554	53	131	0	54.6
105	424.6	1177	623	36.4	90.9	15.9	54.8
106	408	1201	647	55.4	103	0	55
107	408	1232	616	41	103	0	55
108	408	1294	554	41	103	0	56
109	408	1294	554	41	103	0	56
111	476	1294	554	48	120	0	57
112	408	1294	554	41	103	0	58
113	408	1294	554	41	103	0	58
114	408	1232	616	48	103	0	60
115	408	1201	647	41	103	0	63
116	404	1190	640	41	102	16.5	66
117	408	1232	616	41	103	0	66.7
118	476	1294	554	48	120	0	68
119	408	1201	647	41	103	0	68
120	420	1125	750	40	100	0	70.5
121	368	1294	554	53	131	0	71.5
122	404	1190	640	41	102	13.5	76
123	368	1294	554	53	131	0	85.6
124	408	1201	647	41	103	0	89
125	400	950	850	57	143	80	22.6
126	400	950	850	57	143	60	37.3
127	400	950	850	57	143	48	44.8
128	400	950	850	57	143	40	53.5
129	400	1222	658	40	100	0	25
130	400	1222	658	56	84	0	27
131	408	1294	554	41	103	21.3	32
132	408	1294	554	41	103	10.7	35
133	408	1294	554	51.5	103	16.5	36
134	408	1201	647	41	103	20.7	37
135	408	1201	647	41	103	26.5	40
136	408	1294	554	41	103	16.5	40
137	408	1294	554	51.5	103	16.5	41
138	408	1294	554	51.5	103	16.5	41
139	408	1294	554	51.5	103	16.5	42
140	408	1201	647	41	103	14.4	42
141	408	1201	647	41	103	17.6	43
142	408	1294	554	41	103	0	44
143	408	1201	647	41	103	7.5	45
144	408	1201	647	55.4	103	0	44
145	476	1294	554	48	120	0	57
146	408	1201	647	41	103	0	63
147	476	1294	554	48	120	0	68
148	408	1201	647	41	103	0	89
149	408	1246	554	41	103	20	29
150	408	1080	554	41	103	20	29
151	408	1243	554	41	103	20	25
152	408	1232	616	48	103	0	28
153	408	1232	616	41	103	21.3	32
154	408	1232	616	55.4	103	0	33
155	408	1232	616	41	103	10.6	35
156	408	1232	616	41	103	20.7	45
157	408	1232	616	41	103	26.5	48
158	408	1232	616	41	103	14.4	51
159	408	1232	616	41	103	7.5	52
160	408	1232	616	41	103	0	55
161	408	1232	616	41	103	0	66.8
162	420.6	1032	555.7	37.6	80.1	113	33.8
163	350	1200	645	41	103	35	20
164	365.2	1118	602	34.3	73	103	35.3
165	254.5	1290	694.7	22.8	48.5	68.7	36.8
166	309.9	1204	648.4	27.7	59	83.7	42
167	400	1265	540	42.3	105.7	24.3	44
168	405	1235	545	52.9	132.4	28	46
169	380	1233	540	56.5	141.3	14.6	49
170	400	1356	535	51.5	128.6	12.7	52
171	420	1125	750	40	100	0	70.5
172	350	1200	645	41	103	35	48
173	408	1294	554	41	103	22.5	36
174	408	1294	554	41	103	0	56
175	400	950	850	57	144	48	48.5
176	400	1209	651	45.7	114.3	0	26
177	428.6	1177	623	68.6	102.9	28.5	28.6
178	394.3	1201	647	52.6	105.1	21.5	29.7
179	408.9	1177	623	57.2	85.9	24.5	35.7
180	480	1153	599	56	112	23.7	37.1
181	444.4	1177	623	44.4	111.1	18.6	38.7
182	498.5	1153	599	59.8	89.7	26.5	39.9
183	461.5	1177	623	46.2	92.3	18.6	42.5
184	462.9	1153	599	52.9	132.2	21.2	49.6
185	424.6	1177	623	36.4	91	16	54.9
186	406	1194	643	41	102	26.8	37
187	404	1195	640	41	102	20	50
188	408	1294	554	41	103	22.5	45
189	408	1294	554	41	103	0	58
190	408	1201	647	62	93	4	32